Ab initio equation of state for the body-centered-cubic phase of iron at high pressure and temperature

A. B. Belonoshko,[1,*] P. I. Dorogokupets,[2] B. Johansson,[1,3] S. K. Saxena,[4] and L. Koči[3]

[1]*Applied Materials Physics, Department of Material Science and Engineering, The Royal Institute of Technology, SE-10044 Stockholm, Sweden*

[2]*Institute of Earth's Crust, Siberian Branch, Russian Academy of Sciences, Irkutsk, 664033, Russia*

[3]*Condensed Matter Theory, Department of Physics, Box 530, Uppsala University, S-75121 Uppsala, Sweden*

[4]*Florida International University, CeSMEC, University Park, Miami, Florida 33199, USA*

(Received 3 May 2008; revised manuscript received 8 July 2008; published 12 September 2008)

The solid inner core of the Earth consists mostly of iron. There is accumulating evidence that, at the extreme pressures and temperatures of the deep Earth interior, iron stabilizes in the body-centered-cubic phase. However, experimental study of iron at those conditions is very difficult at best. We demonstrate that our *ab initio* approach is capable of providing volumetric data on iron in very good agreement with experiment at low temperature and high pressure. Since our approach treats high-temperature effects explicitly, this allows us to count on similar precision also at high temperature and high pressure. We perform *ab initio* molecular-dynamics simulations at a number of volume-temperature conditions and compute the corresponding pressures. These points are then fitted with an equation of state. A number of parameters are computed and compared with existing data. The obtained equation of state for high pressure and temperature nonmagnetic body-centered-cubic phase allows the computation of properties of iron under extreme conditions of the Earth's inner core.

DOI: 10.1103/PhysRevB.78.104107 PACS number(s): 64.30.Ef, 65.40.−b

I. INTRODUCTION

This paper was motivated by the recent advances in our knowledge of the state of iron under extreme conditions of pressure (P) and temperature (T). In the last fifty years[1–3] it has been established that the Earth has a solid inner core and that the core consists mainly of iron. Understandably, an enormous amount of both experimental and theoretical work was devoted to studies of iron, attempting to measure or compute the properties of iron in the Earth's interior. While the pressures of the Earth's inner core (IC), 3.3–3.64 Mbar, are within reach of advanced experimental studies, the pressures and temperatures (above 4500 K) simultaneously inside the IC remain inaccessible. Shock wave experiments (particularly those with precompressed iron samples) allow the reaching of the conditions of the IC; however, the nature of the emerging phase is not always clear. X-ray *in situ* studies of shock wave compressed samples are not routine yet. So far the equations of state (EOSs) of solid iron under the IC conditions relied mostly on extrapolations of properties measured at pressures and temperatures that are lower than the conditions in the IC.[4]

Let us summarize what is firmly established in this field on the basis of static experiments and what remains to be firmly established. First of all, the low-temperature stable phase of iron is the hexagonal close-packed (hcp) phase.[5] The temperature limit of this phase is not well known. It was demonstrated in a recent work by Ma *et al.*[6] that, up to pressures of 161 GPa and temperatures of up to 3000 K, the hcp phase is stable. With regards to the melting temperature of iron, the study by Ma *et al.*[6] demonstrated that the earlier measurements, which relied on the ability of the naked eye to determine the atomic structure of the emerging phase,[7] are too low and have to be shifted upward by about 700 K (Fig. 1). Note that, however, this is not merely a correction by 700 K at the pressure of 105 GPa. The old measurements[7] positioned the melting point at about 2800 K at 105 GPa. Considering that the melting point of iron at the pressure of 1 bar is 1811 K, the pressure induced increase in the melting temperature (T_m) has been moved up from about 1000 K to 1700 K. That is, the average dT/dP slope of the melting curve increased by about 70%. This is an enormous correction. The

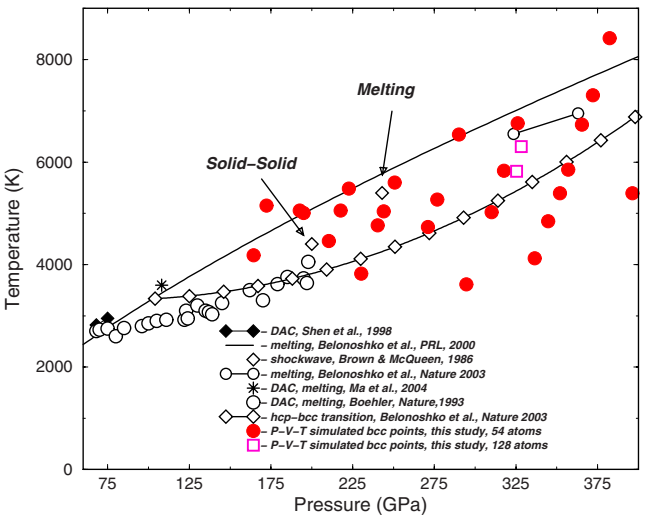

FIG. 1. (Color online) High-pressure iron phase diagram as computed from embedded-atom method tuned to full potential linear-muffin-tin orbitals method (Ref. 8). Continuous curves represent phase boundaries as provided in the legend. The open circles correspond to the low melting curve (Ref. 7), the star is the most recently measured melting temperature (Ref. 6), and the diamonds with error bars are solid-solid and melting transitions. The points where we computed *PVT* points on bcc iron (with 54 atoms supercells) are shown by filled circles. Two open squares show the points, computed with 128 atoms (see text for discussion).

result of Ma *et al.*[6] was in fact predicted in 2000 by Belonoshko *et al.*,[9] while other melting studies, published in about the same time,[10,11] either overestimated[10] or underestimated[11] the melting temperature.

Given that Ma *et al.*'s[6] study was performed with considerably advanced experimental technique compared to the technique in the past century, we gave more credence to their data. Then the questions remains, if not melting, what was observed in the former[7] experiments? One could argue that the temperature measurements had been systematically too low, and that both experimental sets represent melting but with the difference that one study[6] provides correct temperature measurements while the other[7] provides wrong temperature measurements. This is definitely a possibility. However, the melting temperature at the highest pressure of 2 Mbar (Fig. 1) measured so far[7] is coincident (within error bars) with the solid-solid transition observed in the shock wave experiments[12] (recently objected[13] but it is likely that some experimental differences are responsible for the different results). This suggests that the "low" melting curve might in fact represent a solid-solid boundary starting from some (high) pressure (say above 120–150 GPa). Such a hypothesis was tested[8] and, indeed, the transition from hcp to body-centered-cubic (bcc) phase was found (Fig. 1). Since the free energies of the solid Fe phases are extremely close when the temperature approaches melting, different methods produce varying results.[14] However, even when a pure bcc Fe phase comes out unstable, it is admitted that when slightly alloyed by light elements, Fe becomes stable in the bcc phase.[14] Let us now turn to the experimental studies.

Recently, the hcp-bcc transition was observed in Fe alloyed with 10% of Ni at a pressure of 225 GPa and temperatures just above 3400 K.[15] One can see that these conditions are very close to the hcp-bcc boundary as predicted by Belonoshko *et al.*[8] (Fig. 1). Somewhat lower temperature of the experimental transition (3400 K) in comparison to the theoretically predicted[8] temperature (4000 K) is in accordance with the depression due to Ni.[15] The most recent experimental study[16] has found a mixture of hcp and face centered cubic (fcc) in the pure Fe sample, annealed from 160 GPa and 3600 K. Exactly the same mixture is found in Zr if it is quenched from the bcc stability field.[17] Again, these conditions practically coincide with the hcp-bcc phase boundary (Fig. 1) predicted in 2003.[8] While the field for the bcc stability remains to be established, these observations along with the earlier shock wave experiments measuring rarefaction waves velocity behind the shock wave front[12] provide strong evidence in support of the bcc stability in the IC. Besides, assumption of the bcc stability allows one to explain both the low rigidity[18] and anisotropy[19] in the IC.

Thus, the hcp phase of iron might exist nowhere on (or inside) the Earth except within a high-pressure device of an experimentalist. Therefore, it is understandable that an equation of state for the bcc Fe phase at high *PT* has to be established. Such an equation is needed for the following reasons. First, it is of ultimate importance for describing the mechanism, dynamics, and thermodynamics of the IC. The IC is approximately 90% iron; therefore the end member of this alloy, the bcc phase of Fe, has to be described. Second, because an EOS for the hcp phase under the IC conditions exists in many versions, it is of interest to make a comparison between the equations of state for these phases. Third, it is important to provide a correct way for deriving such an equation because previous attempts are not satisfactory due to the reasons explained below.

The paper is organized as follows. In Sec. II we provide a description of the density functional theory (DFT) technique we employed to compute a set of *PVT* (*V* as volume) points for the bcc iron phase. Further, in the same section, we provide a description of the particular EOS we applied to describe the "computer-experimental" data points. In Sec. III we provide the calculated *PVT* data set, provide the parameters of the equation of state, compute a number of important properties of the bcc Fe, and provide their comparative analysis. Some important comments are given in Sec. IV.

II. METHODS

A. *Ab initio* molecular dynamics

The experimental data on the high-*PT* bcc phase are scarce. At room temperature, volumes of hcp iron were measured to 3 Mbar.[5] At the pressure above 2 Mbar, temperatures above 1000 K were reached in internally heated diamond-anvil cells (DACs).[20] The only experimental study that provides data on presumably high-*PT* bcc iron is the shock wave study by Brown and McQueen.[12] The new phase in their experiment was obtained at pressures between 2.0 and 2.4 Mbar at temperatures between 4400 and 5100 K along the Hugoniot adiabat. Therefore, in creating high-*PT* bcc equation of state, we had to rely on the theoretical methods. It was demonstrated that the DFT allows one to compute properties of the hcp Fe phase in reasonable agreement with experimental data.[21] As in the hcp work,[21] we also relied on the projector augmented-wave (PAW) method[22] [as implemented in VASP (Ref. 23)] based on the DFT within the generalized gradient approximation (GGA) using the Perdew-Wang parametrization.[24] The calculations were performed with a cut-off energy of 27 Ry, treating $3p$, $3d$, and $4s$ orbitals as Fe valence states. The choice of valence states is different from the work on hcp Fe;[21] here we do not compromise on their treatment to speed up the calculations. The details of the present calculations are mostly the same as in our recent work on the dynamical stability of iron phases.[25] There are certain differences, however. In all our calculations, supercells of 54 atoms ($3\times3\times3$ multiplication of either bcc or hcp unit cell) have been simulated. We observed that the bcc supercell can be reliably treated with the $2\times2\times2$ k points[26] while the hcp supercell requires the $4\times4\times4$ k-point mesh.

To estimate the precision that we can count on, we computed *PV* data at 0 K for hcp Fe at high pressure. The computed points are shown in Fig. 2. In these calculations we did not optimize the c/a axial ratio but rather have chosen an experimental value close to 1.6. This is to check on the method's performance and to make sure that our setup is not flawed. One can see that the computed points are within the experimental error up to a pressure of about 200 GPa. At higher pressure, some divergence (still moderate) is observed. However, this divergence is not with the original ex-

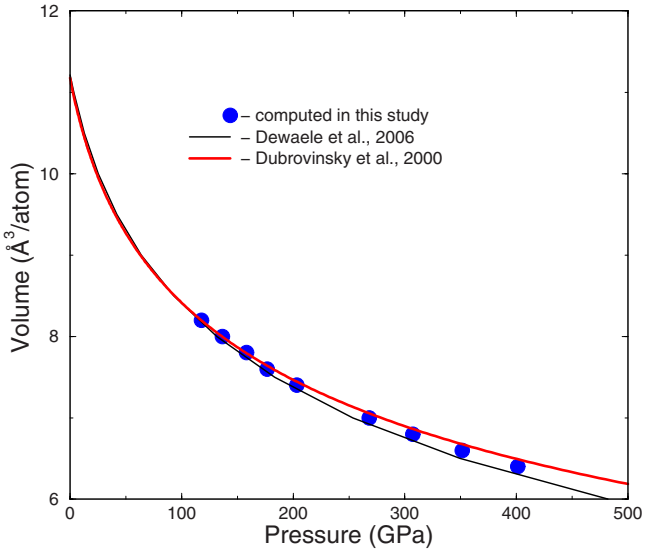

FIG. 2. (Color online) Comparison of two hcp EOS as provided by Dewaele *et al.* (Ref. 27) and Dubrovinsky *et al.* (Ref. 20) with computed, in this work, cold hcp *PV* points.

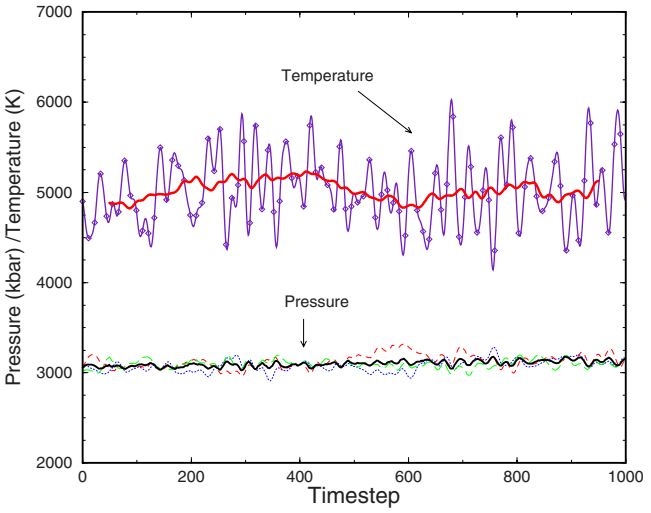

FIG. 3. (Color online) Pressure and temperature time evolutions during a productive stage of molecular-dynamics run for $V=7.0$ Å^3/atom. Pressure curves show the pressure trace (thick continuous curve) as well as P_{xx}, P_{yy}, and P_{zz} components (dotted, dashed, and long-dashed curves) of the pressure tensor. Temperature is shown by the continuous curve with diamonds. The running over 100 time steps average is shown by the thick continuous curve.

perimental data but rather with the Vinet equation[27] that extrapolates data beyond the available experimental pressure range. Considering data from a number of experimental sources, as summarized by Dewaele *et al.*,[27] the computed *PV* points are within the scatter of data. One can see (Fig. 2) that the calculated points fall in between the two[20,27] experimentally based equations of state. This allows us to count on a similar high precision when computing *PVT* data for bcc iron.

We performed *ab initio* molecular dynamics (AIMD) simulations in the *NVE* (*N* as number of atoms, *V* as volume, and *E* as total energy) ensemble. The simulations were performed in the volume range of 6.4–8.0 Å^3/atom. The temperature setting requires, however, some discussion. As has been established by D. M. Sherman,[28] bcc Fe is dynamically unstable at high pressure in the ground state. Therefore, the dynamics of the bcc phase requires very careful treatment. Normally, to control the temperature during an equilibration stage of molecular-dynamics (MD) run, either scaling or some sort of thermostat is applied. Both of these methods interfere with the intrinsic dynamics of a system. Such an interference sometimes might be critical[29,30] because it leads to the destruction of an otherwise dynamically stable structure. In our simulation the velocities have been assigned randomly in the very beginning of the MD run. Thus, if we wanted to perform a simulation at about 3000 K, the initial velocities were assigned to give a kinetic energy corresponding to about twice as large as temperature. This kinetic energy was then spent increasing the potential energy of the system and the rest, after the thermalization (normally a few hundred MD time steps), maintained the temperature at a constant on average level. In this way we minimized the impact of temperature control on the intrinsic dynamics of the bcc structure.

Such a system reaches equilibrium (that is, the stage when intermediate averages do not change) normally within a few hundred time steps. A time step was chosen as 1 fs at lower temperature and 0.5 fs at higher temperatures. This choice was based on our previous experience with AIMD of iron at high *PT*.[8,25] After the equilibration stage, which normally continued for 1000 time steps, we ran AIMD for at least another 1000 time steps to calculate averages.

Figure 3 shows pressure and temperature evolution in a typical MD run. The fluctuations are sufficiently small to provide well constrained averages. The computed *PVT* data is summarized in Table I. Typical statistical errors of MD computed pressures and temperatures are 2.5 GPa and 350 K, respectively. It is important to control the dynamic stability of the bcc phase. To ensure that our system is indeed in the field of dynamic stability, we monitored the hydrostaticity of pressure by controlling the time history of pressure components (Fig. 3). We obtained results consistent with earlier work.[14] Dynamic stability of the bcc phase can be seen above 3000 K. It is possible that the stability sets in at even lower temperature, but in our simulations we tried to avoid runs at temperatures below 3000 K. We know from the molecular-dynamics simulations of Fe with the embedded-atom model[8] that the bcc phase becomes dynamically stable in the range of 1500–3000 K. The dynamical stability sets in at higher temperature upon increasing pressure. The dynamic stability has never been reported below 3000 K in first-principles simulations. Therefore, we restricted our data set by the temperature of 3000 K as the lower limit. At some pressures it is probably possible to decrease the limit. However, to ensure that the fitted set of *PVT* points contains bcc points only, it is wise to set such a limit where the bcc stability is guaranteed.

The impact of comparably small (54) number of atoms was checked by simulations with 128 atoms. These simulations have been performed for the Γ point only because of the high computational cost. However, the convergence was

TABLE I. *PVT* points computed by AIMD.

V (Å^3/atom)	P (GPa)	T (K)
8.0	172.2115	5150.441
8.0	164.3852	4179.249
7.8	192.6674	5052.520
7.8	195.0406	5005.227
7.6	210.4697	4459.617
7.6	217.7082	5052.089
7.6	222.6873	5480.703
7.4	230.1814	3821.912
7.4	240.3826	4765.414
7.4	244.0168	5036.840
7.4	250.8192	5603.485
7.2	271.0351	4734.407
7.2	276.8745	5269.577
7.2	290.0161	6537.439
7.0	294.6674	3613.176
7.0	310.0457	5024.054
7.0	317.5833	5832.551
7.0	326.0204	6756.800
6.8	336.4642	4123.572
6.8	344.7491	4846.771
6.8	351.9267	5394.568
6.8	357.0397	5851.322
6.8	365.4040	6729.252
6.8	372.1253	7307.106
6.8	382.3856	8417.142
6.6	396.3815	5391.348
6.6	409.0708	6678.428
6.6	424.5438	7664.562
6.4	445.9204	5434.729

checked by computing pressures for snapshots with the $2\times2\times2$ k-point mesh. We found that the difference in pressure is small. The 128 atom runs were performed at $V=7.0$ Å^3/atom. The corresponding points are shown in Fig. 1. The same conditions simulated with 54 atoms produce slightly lower (5–7 GPa) pressures. Provided that the pressure is about 320 GPa, this produces error of about 1.5% in pressure. Note that the pressure difference between the experimentally based equations of state (Fig. 2) for hcp phase at 300 GPa is about 10% already at room temperature. Clearly, the impact of small size on our results is reasonably small.

The simulated set is quite comparable in precision to the experimental data on *PVT* data for the bcc phase if such data would have been available. For now, only the shock wave measurements by Brown and McQueen[12] are available. However, temperature was estimated in those experiments from shock Hugoniot thermodynamics and it is difficult to perform a direct comparison. Considering problems with pressure standards, nonhydrostaticity of static ultrahigh-pressure measurements, thermal stress, difficulties of temperature measurements, and possible chemical interactions,

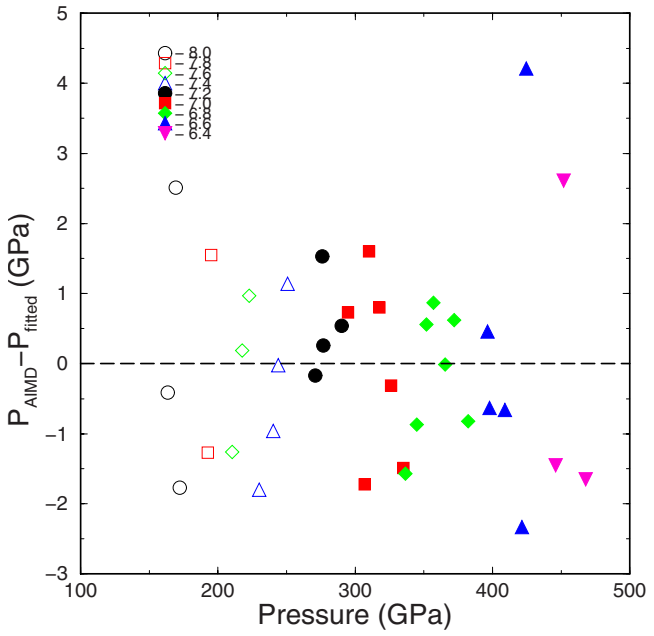

FIG. 4. (Color online) Difference between original (AIMD) computed pressures for the given volumes (see legends; volumes are given in Å^3/atom) and fitted ones. The fitted points are calculated at the corresponding (Table I) temperatures.

to name a few, it is difficult to expect the static experimental data to have the same precision as the measurements of the hcp phase. We see that the *ab initio* calculated *PV* points at low temperature are essentially within the scatter of experimentally based equations of state[22,27] (Fig. 2). Therefore, at high T one can expect that the precision of the computed bcc points would be better than the experimental data because the quality of experimental data quickly deteriorates on increasing temperature at ultrahigh pressure in DAC experiments.

B. Equation of state

Let us write the Helmholtz free energy $F(V,T)$ as the sum[31]

$$F = U_0 + E(V) + F_{\text{th}}(V,T) + F_{\text{anh}}(V,T) + F_{\text{el}}(V,T), \quad (1)$$

where U_0 is the reference energy, $E(V)$ is the potential (cold) part of the free energy on the reference isotherm, which depends only on volume, and $F_{\text{th}}(V,T)$, $F_{\text{anh}}(V,T)$, and $F_{\text{el}}(V,T)$ are the thermal, anharmonic, and electronic contributions, respectively.

Differentiating Eq. (1), we obtain all the necessary thermodynamic functions: entropy $S=-(\partial F/\partial T)_V$, internal energy $E=F+TS$, heat capacity at constant volume, $C_V=(\partial E/\partial T)_V$, pressure, $P=-(\partial F/\partial V)_T$, isothermal bulk modulus, $K_T=-V(\partial P/\partial V)_T$, and the slope of pressure at constant volume $(\partial P/\partial T)_V=\alpha K_T$, where $\alpha=1/V(\partial V/\partial T)_P$. The heat capacity at constant pressure is $C_P=C_V+\alpha^2TVK_T$, and the adiabatic bulk modulus is $K_S=K_T+VT(\alpha K_T)^2/C_V$. The enthalpy and Gibbs energy can be found from $H=E+PV$ and $G=F+PV$.

Here we once again want to emphasize that computation of $E(V)$ for the case of dynamically unstable phases (as is the bcc phase of iron at high pressure) is meaningless. The phase is dynamically unstable if there is a deformation path along which energy of the phase decreases. A dynamically unstable structure, distorted by thermal motion, will transform to another structure spontaneously. All the theories of equation of states assume that we deal with an elastic medium while a dynamically unstable phase is not elastic. There are certain deformations that are not restored when the stress is released. In the case of bcc Fe phase the $E(V)$ term has a meaning as an extrapolated property only. That is, we create the equation at high temperature and then obtain the $E(V)$. This $E(V)$ and the one computed with the flawed assumption on the bcc elasticity[32] are likely to differ. However, from a fundamental point of view it might be of interest to compare such equations. Deriving the $E(V)$ in this work, we answer the question of what could be the "cold" equation of state for bcc Fe if we could extrapolate the EOS to low temperature. The previous work answers the other question, namely: What could be the equation of state for the bcc Fe if we do not pay attention to its dynamical instability? Note that dynamical and thermodynamic instabilities are quite different things. While a thermodynamically unstable but dynamically stable phase can be rightfully treated at any temperature, a dynamically unstable phase cannot be treated at all in the range of dynamical instability. It follows from one simple reason—such a phase simply does not exist; therefore, there is nothing to study.

Lately, the Vinet equation of state[33] has become popular.[27,34,35] In this equation, pressure $P(V)$ can be written as

$$P(V) = \partial E/\partial V = 3K_0 y^{-2}(1-y)\exp[(1-y)\eta], \tag{2}$$

where $y = x^{1/3} = (V/V_0)^{1/3}$ and $\eta = 1.5(K'-1)$, $K' = dK/dP$, and V_0 and K_0 are molar volume and bulk modulus at reference conditions ($T_0 = 298.15$ K and $P_0 = 1$ bar).

The Vinet EOS (Ref. 33) is often criticized (e.g., Ref. 36) although up to compressions of about 0.6 the Vinet *et al.*'s[33] and Holzapfel *et al.*'s[36] EOSs are close.

We decided to employ the Holzapfel equation in the form

$$P(V) = 3K_0 X^{-5}(1-X)\exp[c_0(1-X)][1+c_2 X(1-X)], \tag{3}$$

where $X = (V/V_0)^{1/3}$, $c_0 = -\ln(3K_0/P_{\mathrm{FG0}})$, $P_{\mathrm{FG0}} = 1003.6(Z/V_0)^{5/3}$, and $c_2 = 3/2(K'-3) - c_0$. The units of V_0 are cm^3/mole, and units of P_{FG0} are GPa. This equation provides us with a correct Thomas-Fermi limit of pressure at infinite compression.[37]

For the quasiharmonic term in Eq. (1) we have chosen the Einstein approximation, which, in the range of the considered pressures and temperatures, practically coincides with the Debye model. These formulas are well known but we write them here for completeness:

$$F_{\mathrm{th}} = 3nR\left[\frac{\Theta}{2} + T\ \ln\left(1-\exp\frac{-\Theta}{T}\right)\right]. \tag{4}$$

Here Θ is the Einstein temperature, R is gas constant, and n is number of atoms, which is here equal to one. Then

$$S_{\mathrm{th}} = 3nR\left\{\ln\left[1-\exp\left(\frac{\Theta}{T}\right)\right] - \frac{\Theta/T}{\exp(\Theta/T)-1}\right\}, \tag{5}$$

$$E_{\mathrm{th}} = 3nR\left[\Theta/2 + \frac{\Theta}{\exp(\Theta/T)-1}\right], \tag{6}$$

and

$$C_{V\mathrm{th}} = 3nR(\Theta/T)^2\frac{\exp(\Theta/T)}{[\exp(\Theta/T)-1]^2}. \tag{7}$$

Thermal pressure can be obtained by taking the derivative of the free energy on volume at constant temperature, $P_{\mathrm{th}} = -(\partial F_{\mathrm{th}}/\partial V)_T$:

$$P_{\mathrm{th}} = \gamma E_{\mathrm{th}}/V, \tag{8}$$

where $\gamma = -(\partial\ \ln\ \Theta/\partial\ \ln\ V)_T$.

The isothermal bulk modulus follows from the relation $K_{T\mathrm{th}} = -V(\partial P_{\mathrm{th}}/\partial V)_T$,

$$K_{T\mathrm{th}} = P_{\mathrm{th}}(1+\gamma-q) - \gamma^2 T C_{V\mathrm{th}}/V, \tag{9}$$

where $q = (\partial\ \ln\ \gamma/\partial\ \ln\ V)_T$.

For the volume dependence of the Grüneisen parameter, we used Al'tshuler *et al.*'s[38] form:

$$\gamma = \gamma_\infty + (\gamma_0 - \gamma_\infty)(V/V_0)^\beta = \gamma_\infty + (\gamma_0 - \gamma_\infty)x^\beta, \tag{10}$$

where γ_0 is the Grüneisen parameter at ambient conditions, γ_∞ is the Grüneisen parameter at infinite compression ($x = 0$), and β is a fitted parameter. The form (10) is simple and convenient, has a correct asymptotic behavior at $x \to 0$, and, in our experience, it describes extremely well the results of theoretical calculations. From Eq. (10) it is possible to calculate the volume dependence of the characteristic temperature (here we use the same γ for all frequencies):

$$\Theta = \Theta_0 x^{-\gamma_\infty}\exp\left[\frac{\gamma_0 - \gamma_\infty}{\beta}(1-x^\beta)\right]. \tag{11}$$

Overall, this is a very reasonable approximation for the Grüneisen parameter and at the same time very flexible. For compressions higher than 0.5, the behavior of the Grüneisen parameter might be complicated.[36] Therefore, we should not attempt to use Eq. (10) above that compression. Al'tshuler *et al.*[38] suggested using $\beta = \gamma_0/(\gamma_0 - \gamma_\infty)$. This expression was successfully applied to describe properties of hexagonal iron.[27] In this study β is a fitting parameter.

In our model the intrinsic anharmonicity term of the Helmholtz free energy is presented in the simplest possible form,[31]

$$F_a(V,T) = -\frac{3}{2}nRaT^2 = -\frac{3}{2}nRa_0 x^m T^2, \tag{12}$$

where $n = 1$ (monatomic substance).

Correspondingly, the pressure due to the anharmonicity becomes

$$P_{\mathrm{a}} = \frac{3}{2}nRa\frac{m}{V}T^2. \tag{13}$$

TABLE II. Comparison of bulk moduli for bcc iron.

T (K)	P (GPa)	K_T (GPa) Ref. 39	K_T (GPa) This work
750	133.23	841	764
1500	139.76	832	766
2250	146.67	830	770
5500	304.36	1275	1251
2000	337.32	1540	1471
4000	358.17	1515	1483
6000	379.36	1473	1497

The electronic entropy term can be accounted in the same way. However, since the functional dependence on T for a given V is identical with the anharmonicity, we combine two terms in one. Therefore, this anharmonic term becomes a cumulative one, accounting for both anharmonicity and electronic entropy.

It would be perhaps more correct to choose the T_0 as the temperature of the dynamic stability onset. Our choice of room temperature as the T_0 is explained by tradition and convenience. It might be dangerous to rely on the cold bcc equation as having an independent physical meaning. The cold equation of state here is nothing but an extrapolation of high-PT data to low temperature.

III. RESULTS AND DISCUSSION

Parameters of the equation of state were obtained by minimizing the difference between the volumes computed from Eqs. (5)–(13) at the corresponding P and T (Table I), and the volumes at which AIMD simulations have been performed. The minimization was performed by the least square method. This fitting resulted in the following parameters: $V_0=6.5021$ cm^3/mole, $K_0=198.07$ GPa, $K'=5.426$, $\Theta_0=628$ K, $\gamma_0=2.052$, $\beta=0.701$, and $\gamma_\infty=0.91$. We found that the term proportional to T^2 is very small, and, therefore, the cumulative electronic and anharmonicity term was assumed to be zero. The standard deviation of volume and pressure was 0.12% and 1.44 GPa, respectively. The quality of the fit is illustrated by Fig. 4. The differences between the original AIMD PVT data and that computed from the EOS are at most 1% in pressure, which is very good by any standard. Experimental error is a few percent in pressure even at low temperatures. We do not see any systematic error in the quality of fitting. This suggests that the model is adequate and that the major source of error is likely the statistical error of the molecular dynamics averaging.

We can compare the results of fitting with previous calculations of K_T.[39] Pressure is computed with V_0 in this work (6.5021 cm^3/mole). The agreement seems to be quite reasonable (Table II) although at low pressure and temperature the bulk modulus in this work is somewhat higher. There are several reasons for the difference. First, the difference is the largest (up to 10%) at low temperature (750 and 1500 K) at comparably low pressure. This PT range is outside of the PT range of our AIMD simulations. Second, bulk moduli in Ref. 39 are computed in isolated points while in our equations they are constrained by large set of points. The major reason for disagreement is likely extrapolation: as soon as we compare bulk moduli in the range of our AIMD simulations (lines 4, 6, and 7 in Table II), the agreement is very good. Another comparison can be done with the shock wave data by Brown and McQueen.[12] This is essentially the only experiment that provides PVT data on the bcc phase at high pressure and temperature. According to experiment, the density of the emerging phase at the pressure of 240 GPa and temperature of 5100 K (right before melting in the shock wave experiment) is equal to 12.31 ± 0.07 g/cm^3. At this pressure and temperature, our equation of state gives a density of 12.48 g/cm^3. Considering errors of our procedure and error bars of the experiment, the agreement is good.

Figures 5(a)–5(d) show a comparison of several properties as calculated with our equation and the one developed by Dewaele *et al.*[27] While direct comparison between the equations should be performed with caution, we see certain features that warrant discussion. Most remarkably, we do not see much curvature in change of the bulk modulus with temperature. It follows straightforwardly from the low anharmonicity of the bcc phase. This is counterintuitive because the bcc phase was thought to be stabilized (dynamically) by anharmonicity. Also, this is different from the case of hcp Fe (Ref. 40) where large electronic and anharmonic effects are expected. While an elaborated explanation of such behavior of bcc phase requires a separate study, there is an explanation that seems to us plausible. Unlike hcp phase, bcc phase is dynamically unstable up to about 3000 K. Therefore, the temperature of 3000 K, which is rather high for hcp phase, for bcc phase is equivalent to the starting temperature. Similarly, temperature of 7000 K, where we see significant anharmonicity in hcp phase, is effectively just 4000 K above the onset of dynamical stability in bcc phase. We do not see much curvature in hcp isochores until temperature rises above 3000 K. Similarly, we probably should not expect to see this curvature for the bcc phase. In a dynamically unstable structure, there is a room for thermal motion without exciting anharmonicity. Similarly, occupancy of higher electronic states on increasing temperature should be preceded by the changes of electronic structure to make the atomic structure dynamically stable first. In our simulations we compute density of electronic states. However, for the purpose of this work, explanation for the particular behavior of electronic structure with temperature is irrelevant. Whether explained or not, equation of state shall not change. Such an explanation is a subject of a separate study, similar to the one recently performed for Mo.[41] We note that, however, a nearly harmonic behavior of the bcc phase is against expectations. If the bcc phase becomes more stable than the hcp phase[8] then this is likely due to the very fact of the bcc dynamic instability at low temperature rather than due to the bcc anharmonicity.

We want to make one rather general remark. It is only recently that the need in EOSs for phases that are dynamically unstable at low T has emerged. Therefore, the theory behind dynamical stabilization has not yet been fully developed. It could be that the model we use does not reflect the physics behind the bcc phase stabilization. It would be more

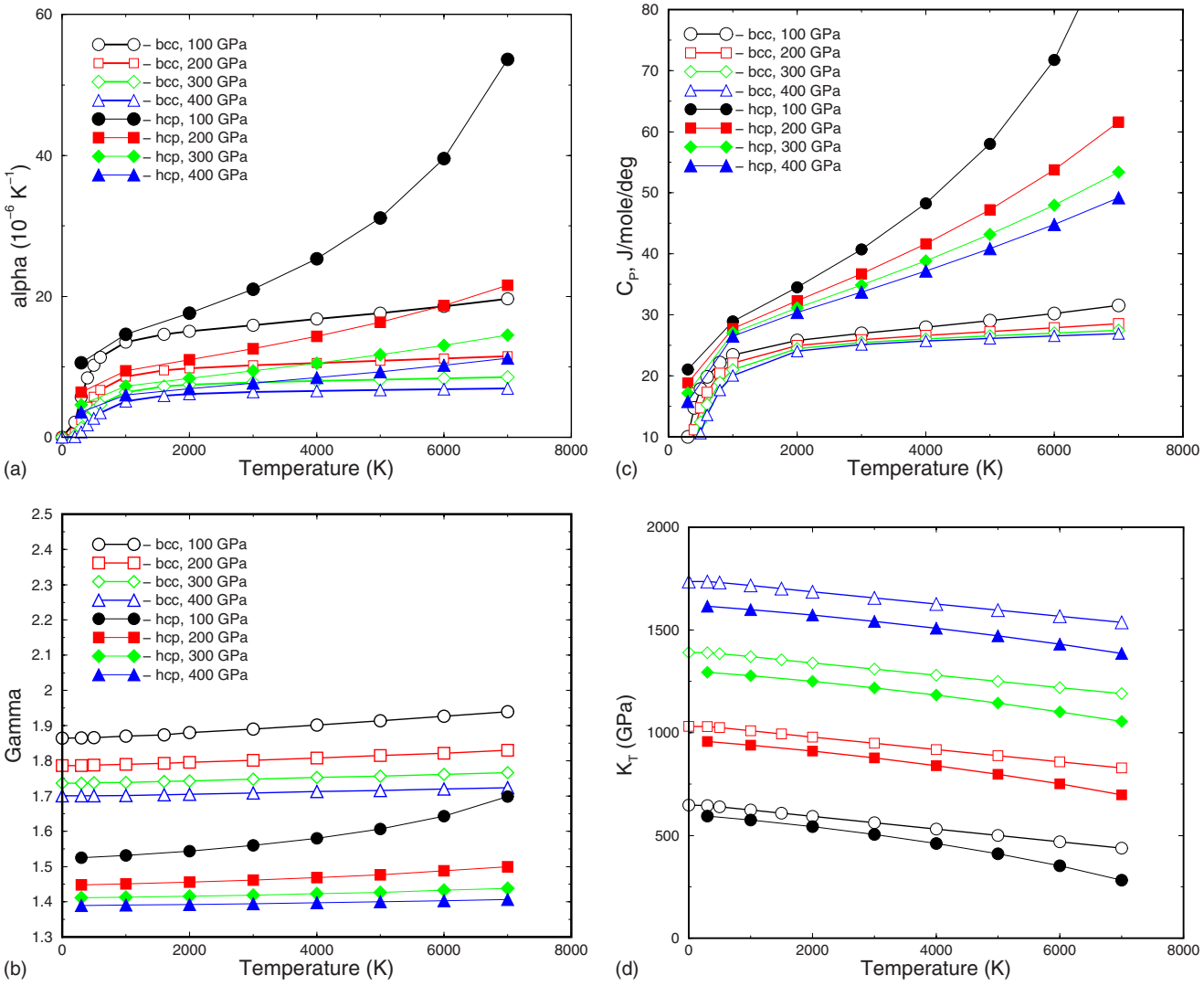

FIG. 5. (Color online) Properties of the bcc phase (this work) (thick curves with open symbols) compared to hcp phase (Ref. 27) (thin curves with filled symbols). (a) Thermal expansion coefficient; (b) Grüneisen parameter γ; (c) heat capacity at constant pressure; (d) bulk modulus. Comparison is provided at 4 pressures: 100, 200, 300, and 400 GPa as a function of temperature. Note the field of stability of bcc and hcp phases (Fig. 1).

safe to consider the model as the equation that allows interpolation and to some extent extrapolation of the computed with AIMD data.

Considering that bcc iron is likely to be the material in the core, it is of interest to summarize the computed properties for that phase (Table III). The properties are computed at the pressure of 364 GPa, which is the pressure in the center of the Earth.

The temperature of melting of pure iron in the center of the Earth, that is, at the pressure of 364 GPa, can be rather

TABLE III. Thermodynamic properties of bcc iron at the pressure of 364 GPa.

T (K)	V (cm^3/mole)	α (10^{-6} K^{-1})	C_P (J mol^{-1} K^{-1})	K_T (GPa)	γ
2000	3.9645	6.56	24.206	1563.4	1.718
3000	3.9913	6.86	25.245	1533.2	1.722
4000	4.0191	7.04	25.829	1503.3	1.726
5000	4.0478	7.18	26.286	1473.5	1.730
5500	4.0624	7.24	26.495	1458.7	1.732
6000	4.0772	7.31	26.698	1443.9	1.734
6500	4.0922	7.37	26.898	1429.2	1.736
7000	4.1074	7.43	27.097	1414.5	1.738

reliably set around 7000 K. This estimate is within the error bars of the two theoretical predictions.[9,10] It is slightly higher than the empirical (which does not include the latest high melting point[6]) estimate of 6600 K. It is significantly higher than the temperature based on extrapolations of Boehler's[7] melting data. The estimate of 7000 K is also significantly lower than the temperature provided in earlier studies.[42] Considering, that the theoretical method in Ref. 9 correctly predicts the latest experimental melting temperatures,[6] it is a natural choice to rely on at the higher pressure.

At this temperature, density of Fe at the pressure of 364 GPa (Table III) is about 13.59 g/cm^3, which can be compared to the density in the center of the Earth (13.09 g/cm^3) according to the Preliminary Reference Earth model.[43] If alloying Fe does not change its volume (which is rather realistic at very high pressures), and a typical impurity is close to Si in molecular weight,[2] then about 7.5% of impurities will suffice to match the observed density in the center of the Earth. This estimate will decrease with molecular weight of an impurity and will increase on decreasing temperature.

IV. CONCLUSIONS

Summarizing, we have provided a theoretical equation of state for nonmagnetic bcc Fe under extreme conditions of pressure and temperature, typical of the Earth's inner core. We performed simulations at the highest presently available theory level. However, we see room for improvement. First, we expect that a theoretical model of an equation of state will be developed for phases that are dynamically unstable at low temperature. Such a development would allow us to rely on the physical meaning of parameters in the equation of state. At present, we suggest using these parameters with caution. Second, we would like to see simulations for larger computational cells to account for anharmonicity and low-frequency phonons more precisely. We do not expect any drastic improvements in the EOS. However, because Gibbs energies of open and close-packed phases are extremely close when approaching melting temperatures, it might be important for calculations of their relative thermodynamic stability. With this equation of state now available, we can put the thermodynamic computing of iron in the IC on the solid quantitative basis.

ACKNOWLEDGMENTS

Computations were performed at the National Supercomputer Center in Linköping and the Parallel Computer Center in Stockholm. A.B.B. appreciates the hospitality of CeSMEC during this work. P.I.D. thanks the Russian Foundation for Basic Research for financial support (Project No. 06-05-64579). We also thank the Swedish Research Council (VR) and the Swedish Foundation for Strategic Research (SSF) for financial support.

*anatoly@fysik.uu.se

[1] I. Lehmann, Bur. Cent. Seismol. Int. **14**, 3 (1936).
[2] F. Birch, J. Geophys. Res. **57**, 227 (1952).
[3] L. V. Altshuler, K. K. Krupnikov, B. N. Lebedev, V. I. Zhuchikhin, and M. I. Brazhnik, Zh. Eksp. Teor. Fiz. **34**, 874 (1958).
[4] R. J. Hemley and H.-K. Mao, Int. Geol. Rev. **43**, 1 (2001).
[5] H.-K. Mao, Y. Wu, L. C. Chen, J. F. Shu, and J. P. Jephcoat, J. Geophys. Res. **95**, 21737 (1990).
[6] Y. Ma, M. Somayazulu, G. Shen, H. K. Mao, J. Shu, and R. Hemley, Phys. Earth Planet. Inter. **143-144**, 455 (2004).
[7] R. Boehler, Nature (London) **363**, 534 (1993).
[8] A. B. Belonoshko, R. Ahuja, and B. Johansson, Nature (London) **424**, 1032 (2003).
[9] A. B. Belonoshko, R. Ahuja, and B. Johansson, Phys. Rev. Lett. **84**, 3638 (2000).
[10] D. Alfé, M. J. Gillan, and G. D. Price, Nature (London) **401**, 462 (1999).
[11] A. Laio, S. Bernard, G. L. Chiarotti, S. Scandolo, and E. Tosatti, Science **287**, 1027 (2000).
[12] J. M. Brown and B. G. McQueen, J. Geophys. Res. **91**, 7485 (1986).
[13] J. H. Nguyen and N. C. Holmes, Nature (London) **427**, 339 (2004).
[14] L. Vocadlo, D. Alfe, M. J. Gillan, I. G. Wood, J. P. Brodholt, and G. D. Price, Nature (London) **424**, 536 (2003).
[15] L. S. Dubrovinsky, N. Dubrovinskaia, O. Narygina, I. Kantor, A. Kuznetzov, V. B. Prakapenka, L. Vitos, B. Johansson, A. S. Mikhaylushkin, S. I. Simak, and I. A. Abrikosov, Science **316**, 1880 (2007).
[16] A. S. Mikhaylushkin, S. I. Simak, L. Dubrovinsky, N. Dubrovinskaia, B. Johansson, and I. A. Abrikosov, Phys. Rev. Lett. **99**, 165505 (2007).
[17] U. Pinsook, Phys. Rev. B **66**, 024109 (2002).
[18] A. B. Belonoshko, N. V. Skorodumova, S. Davis, A. N. Osiptsov, A. Rosengren, and B. Johansson, Science **316**, 1603 (2007).
[19] A. B. Belonoshko, N. V. Skorodumova, A. Rosengren, and B. Johansson, Science **319**, 797 (2008).
[20] L. S. Dubrovinsky, S. K. Saxena, F. Tutti, S. Rekhi, and T. LeBehan, Phys. Rev. Lett. **84**, 1720 (2000).
[21] D. Alfè, G. D. Price, and M. J. Gillan, Phys. Rev. B **64**, 045123 (2001).
[22] P. E. Blöchl, Phys. Rev. B **50**, 17953 (1994).
[23] G. Kresse and J. Furthmüller, Comput. Mater. Sci. **6**, 15 (1996); Phys. Rev. B **54**, 11169 (1996); G. Kresse and D. Joubert, *ibid.* **59**, 1758 (1999).
[24] J. P. Perdew, J. A. Chevary, S. H. Vosko, K. A. Jackson, M. R. Pederson, D. J. Singh, and C. Fiolhais, Phys. Rev. B **46**, 6671 (1992).
[25] A. B. Belonoshko, E. I. Isaev, N. V. Skorodumova, and B. Johansson, Phys. Rev. B **74**, 214102 (2006).
[26] H. J. Monkhorst and J. D. Pack, Phys. Rev. B **13**, 5188 (1976).
[27] A. Dewaele, P. Loubeyre, F. Occelli, M. Mezouar, P. I. Dorogokupets, and M. Torrent, Phys. Rev. Lett. **97**, 215504 (2006).

[28] D. M. Sherman, *High-Pressure Science and Technology–1993*, AIP Conf. Proc. No. 309 (AIP, Woodbury, NY, 1994), p. 895.
[29] A. B. Belonoshko, N. V. Skorodumova, A. Rosengren, and B. Johansson, Phys. Rev. B **73**, 012201 (2006).
[30] A. B. Belonoshko, S. Davis, N. V. Skorodumova, P. H. Lundow, A. Rosengren, and B. Johansson, Phys. Rev. B **76**, 064121 (2007).
[31] V. N. Zharkov and V. A. Kalinin, *Equations of State of Solids at High Pressures and Temperatures* (Consultants Bureau, New York, 1971).
[32] P. Modak, A. K. Verma, R. S. Rao, B. K. Godwal, and R. Jeanloz, J. Mater. Sci. **41**, 1523 (2006).
[33] P. Vinet, J. Ferrante, J. Rose, and J. Smith, J. Geophys. Res. **92**, 9319 (1987).
[34] P. I. Dorogokupets and A. Dewaele, High Press. Res. **27**, 431 (2007).
[35] A. Dewaele, F. Datchi, P. Loubeyre, and M. Mezouar, Phys. Rev. B **77**, 094106 (2008).
[36] W. B. Holzapfel, M. Hartwig, and W. Sievers, J. Phys. Chem. Ref. Data **30**, 515 (2001); W. B. Holzapfel, Z. Kristallogr. **216**, 473 (2001); W. B. Holzapfel and M. Nicol, High Press. Res. **27**, 377 (2007).
[37] W. B. Holzapfel, Rep. Prog. Phys. **59**, 29 (1996).
[38] L. V. Al'tshuler, S. E. Brusnikin, and E. A. Kuz'menkov, J. Appl. Mech. Tech. Phys. **28**, 129 (1987).
[39] L. Voĉadlo, Earth Planet. Sci. Lett. **254**, 227 (2007).
[40] D. A. Boness, J. M. Brown, and A. K. McMahan, Phys. Earth Planet. Inter. **42**, 227 (1986).
[41] C. Asker, A. B. Belonoshko, A. S. Mikhaylushkin, and I. A. Abrikosov, Phys. Rev. B **77**, 220102(R) (2008).
[42] Q. Williams, E. Knittle, and R. Jeanloz, J. Geophys. Res. **96**, 2171 (1991).
[43] A. M. Dziewonski and D. L. Anderson, Phys. Earth Planet. Inter. **25**, 297 (1981).